

Violent relaxation in one-dimensional self-gravitating system: deviation from the Vlasov limit due to finite- N effect

Tirawut Worrakitpoonpon*

Institute of Science, Suranaree University of Technology, Nakhon Ratchasima 30000, Thailand

(Dated:)

We investigate the effect of a finite particle number N on the violent relaxation leading to the Quasi-Stationary State (QSS) in a one-dimensional self-gravitating system. From the theoretical point of view, we demonstrate that the local Poissonian fluctuations embedded in the initial state give rise to an additional term proportional to $1/N$ in the Vlasov equation. This term designates the strength of the local mean-field variations by fluctuations. Because it is of the mean-field origin, we interpret it differently from the known collision term in the way that it effects the violent relaxation stage. Its role is to deviate the distribution function from the Vlasov limit, in the collisionless manner, at a rate proportional to $1/N$ while the violent relaxation is progressing. This hypothesis is tested by inspecting the QSSs in simulations of various N . We observe that the core phase-space density can exceed the limiting density deduced from the Vlasov equation and its deviation degree is in accordance with the $1/N$ estimate. This indicates the deviation from the standard mean-field approximation of the violent relaxation process by that $1/N$ term. In conclusion, the finite- N effect has a significant contribution to the QSS apart from that it plays a role in the collisional stage that takes place long after. The conventional collisionless Vlasov equation might not be able to describe the violent relaxation of a system of particles properly without the correction term of the local finite- N fluctuations.

I. INTRODUCTION

Long-range interacting systems constitute a major branch in statistical mechanics and attract much interest due to their complex nature (see [1] for review). In general, an out-of-equilibrium state evolves first through a stage of violent relaxation in which the dynamics is governed by a self-consistent mean field with a time scale of the order of dynamical times. This stage is otherwise known as the collisionless evolution due to the lack of the collisional interaction between the particles. That collisionless dynamics during that stage can be described by the Vlasov equation. At the end of the violent relaxation, the system settles into a the Quasi-Stationary State (QSS). A descriptions of the violent relaxation and the resulting QSS have been proposed by Lynden-Bell (hereafter LB) [2], initially aiming to explain the inconsistency between the light distribution of an elliptical galaxy and the isothermal sphere profile that is the thermal equilibrium analogue for the three-dimensional self-gravitating system. That work estimated the violent relaxation time scale by the rate of change of the mean field and proved that the time scale was of the order of dynamical times regardless of the system's physical parameters. This allows a galaxy to be established as a QSS within a time scale shorter than the age of the Universe. The statistical description of the QSS differs from the thermal equilibrium which represents a state of maximized Boltzmann entropy. Since then, the LB theory has become a central pillar in the field of astrophysics and the studies of systems governed by long-range interactions.

While the Vlasov equation addresses the collisionless evolution of the long-range interacting systems in the fluid limit, the violent relaxation is mostly investigated using systems of particles in which the time integration of the particle dynamics is simple compared to the direct integration of the Vlasov equation. However, the Poissonian fluctuations embedded in particle systems must be properly considered. A finite particle number N constitutes the collision term proportional to $1/N$ that arises from the two-point correlation function in the BBGKY hierarchy [3–5]. It introduces a collisional effect to the QSS and drives it to thermal equilibrium with a time scale increasing with N as verified in the one-dimensional self-gravitating system [6–8] and the Hamiltonian Mean-Field (HMF) model [9, 10]. Although the knowledge of the finite- N effect on the long-term evolution to the thermal equilibrium is well established theoretically and numerically, its impact on the preceding violent relaxation is not well investigated. Studies of the HMF model have mentioned the finite- N effect on the QSS with a deviation of the QSS from the prediction based on the fluid limit [11–14]. The finite- N effect has also been addressed for a system with attractive power-law interaction and the correction term to the Vlasov equation was required in order to describe the particle dynamics properly [15]. The N -dependence of the QSS is interesting since it was not described by the original LB theory which considered the fluid analogue. Although the finite- N effect was not taken into account, the LB theory was shown to be applicable in a limited number of situations. In most cases, the systems underwent incomplete relaxation that prevented them to achieve the LB configuration [16–20].

The main purpose of this study is to better understand, theoretically and numerically, the involvement of the finite- N effect in the violent relaxation and the result-

* Corresponding author: worraki@gmail.com

ing QSS in the one-dimensional self-gravitating system. The article is organized as follows. In Sec. II, the analysis of the Vlasov equation that incorporates the local Poissonian fluctuations is performed and the relevance to the finite- N QSS is discussed. Sec. III details of the initial condition for the simulations, the units, and the simulation method. In Sec. IV, the numerical results and the comparison with the theoretical framework are presented. Finally, Sec. V concludes this study.

II. ANALYSIS OF THE VLASOV EQUATION WITH LOCAL FLUCTUATIONS

We recall the Vlasov equation that governs the collisionless evolution of the distribution function $f(\mathbf{x}, \mathbf{v})$

$$\frac{df}{dt} = \frac{\partial f}{\partial t} + \mathbf{v} \cdot \frac{\partial f}{\partial \mathbf{x}} + \mathbf{a} \cdot \frac{\partial f}{\partial \mathbf{v}} = 0 \quad (1)$$

where \mathbf{a} is the self-consistent mean-field acceleration, an acceleration from all phase-space elements of the system, derived from the gradient of the mean-field potential Φ as

$$\mathbf{a}(\mathbf{x}) = -\nabla_{\mathbf{x}}\Phi. \quad (2)$$

By definition, Φ can be written in terms of the integral of f as

$$\Phi(\mathbf{x}) = \int \int \varphi(\mathbf{x}, \mathbf{x}') f(\mathbf{x}', \mathbf{v}') d\mathbf{x}' d\mathbf{v}' \quad (3)$$

where $\varphi(\mathbf{x}, \mathbf{x}')$ is the pair potential at \mathbf{x} from the mass element at \mathbf{x}' . According to the LB analysis [2], there are two types of system distribution functions: the fine-grained and the coarse-grained distribution functions. The former one represents the phase-space density of a system segmented into smallest divisible phase-space elements, or microcells, each of which is so small that we can approximate its density to be uniform and non-zero inside when occupied and zero otherwise. The latter one is the average of the phase-space density inside a macrocell, a cell that consists of multiple microcells. The statistical equilibrium is attainable on the coarse-grained level, whereas the fine-grained level never attains because fine-grained entropy does not increase. Throughout this section, all distribution functions are the coarse-grained ones. In simulation aspect, the measured distribution function and the other profiles derived from it can be considered as coarse-grained properties as they are computed with a finite bin size.

If $f(\mathbf{x}, \mathbf{v})$ denotes the point-wise one-particle distribution function, Eq. (1) is known as the Klimontovich equation. In the case of Newtonian gravity, Eq. (1) is coupled with the Poisson equation and these equations are called collectively the Vlasov-Poisson equations. For an initial state consisting of N particles, we express the system distribution function f in the form

$$f = \bar{f} + \delta f, \quad (4)$$

where the first term corresponds to the distribution function in fluid limit and the second term represents the local variation due to the Poissonian fluctuations (see [1] for review). The variation term vanishes by ensemble average, i.e., $\langle \delta f \rangle = 0$, so $\langle f \rangle$ converges to \bar{f} . In statistical sense, the ensemble average of a quantity or a function can be obtained by averaging it over infinite number of realizations starting with initial conditions sampled from the same distribution function. In practice, the ensemble average over hundreds of realizations is found sufficient for reliable distribution functions of the QSSs. The fluctuations of f lead to the fluctuations of the mean-field acceleration $\delta\mathbf{a}$ accordingly, i.e., $\mathbf{a} = \bar{\mathbf{a}} + \delta\mathbf{a}$ where $\bar{\mathbf{a}}$ is the mean-field acceleration from \bar{f} . From Eqs. (3) and (4), we can deduce that $\delta\mathbf{a}$ is an integral of δf which vanishes after averaging in the same way as δf . All variation terms are scaled by $1/\sqrt{N}$ as they originate from the Poissonian noise. By substituting the perturbed quantities into Eq. (1) and performing the ensemble average, the perturbed Vlasov equation becomes

$$\left\langle \frac{d\bar{f}}{dt} \right\rangle = -\left\langle \delta\mathbf{a} \cdot \frac{\partial \delta f}{\partial \mathbf{v}} \right\rangle \sim \frac{1}{N}, \quad (5)$$

where

$$\frac{d\bar{f}}{dt} = \frac{\partial \bar{f}}{\partial t} + \mathbf{v} \cdot \frac{\partial \bar{f}}{\partial \mathbf{x}} + \bar{\mathbf{a}} \cdot \frac{\partial \bar{f}}{\partial \mathbf{v}}. \quad (6)$$

Although the ensemble average eliminates all terms involving first-order fluctuations in Eq. (5), a non-vanishing second-order term proportional to $1/N$ remains, which is of the mean-field origin and embedded in the initial state. This analytical result may appear at first analogous to the one obtained from the quasi-linear analysis from which the $1/N$ term is recognized as the collision term [21, 22]. In this work, however, we interpret the role of this term and its intrinsic properties differently. Conventional analysis expresses the two perturbative terms on the right-hand side in forms of the spatio-temporal Fourier transforms of δf , and the ensemble average of their product corresponds to the spatio-temporal two-point correlation function. This is the result derivable from the standard Lenard-Balescu equation [23]. We have an alternative view on that term starting from a simple dynamical perspective that $\delta\mathbf{a}$ which involves the integral of δf over the entire phase space, designates how large the local fluctuation of mean-field acceleration is at any location. The product $\delta f \delta\mathbf{a}$ in that term can then be regarded as the local fluctuations of accelerations amplified by local variations δf , which can also be interpreted as the strength of the deviation from mean-field approximation. As the seed of this term, namely $\delta\mathbf{a}$, is of mean-field origin, we hypothesize that it is associated with the collisionless relaxation to the QSS rather than the collisional relaxation to thermal equilibrium. Broadly speaking, this term can be considered as the mean-field correction term in the Vlasov equation due to finite N . The violent relaxation incorporating this term can be described as follows. In a finite- N system, there exists

the mean-field fluctuations with amplitudes proportional to $1/\sqrt{N}$ in addition to the mean field from the fluid limit. This combined mean field self-consistently governs the early dynamics altogether and it deviates the distribution function \bar{f} from the Vlasov limit at a rate proportional to $1/N$. The N -dependence arising from the proposed term, which is of mean-field origin, is unlike the N -dependent collisional effect that involves the two-point correlation and comes into play much later. The proposed mechanism is therefore a distinct process from the collisional evolution. Because the violent relaxation time scale does not depend on N , the accumulated deviation at the end is expected to scale with $1/N$. In other words, such effect manifests the N -dependence of the QSS which is not foreseen by the original LB theory. The $1/N$ term can otherwise be regarded as the mean-field correction term of the Vlasov equation when considering finite- N systems. As for the collision term, this fluctuation term vanishes as $N \rightarrow \infty$. In that limit, the evolution follows strictly the Vlasov equation, i.e., $df/dt = d\bar{f}/dt = 0$. This happens when one directly solves the Vlasov equation for the evolution of f , either numerically or semi-analytically [24–29]. Note that this estimate of the $1/N$ term is valid for any long-range interacting systems as long as the Poissonian fluctuations are present. Although applying the perturbative analysis to the Vlasov equation yields the analytical results that are analogous, in a broad sense, to those involving the collision term from the BBGKY hierarchy, the scope of the applicability of our analysis is more limited. Most importantly, the violent relaxation, which is our focus here, leads to the QSS that differs greatly from the initial state in most of the cases and the system evolves rapidly in a short time scale. The full perturbative analysis therefore fails to be valid. As a matter of fact, our analysis only provides an estimate of the rate of the departure from the Vlasov limit starting from the non-equilibrium initial condition, via the analysis that yields lastly Eq. (5). We do not provide a full description of how the perturbation (or δf) evolves, nor how the final QSS appears. On the contrary, the collisional term drives the QSS slowly and quasi-statically through the series of the dynamical equilibria in the course of the thermalization and the system eventually attains thermal equilibrium.

In a confined system such as the HMF model, the term δf can be assumed to take a form of the standing wave. A recent work by [22] performed the quasi-linear analysis in that way and investigated its effect on the QSS. The results were compared with N -body simulations and it was found that the analysis was applicable in a certain range of energy. Otherwise, a large deviation from the theory was found. It may appear that the starting point and the purpose of this work are similar to ours: the perturbative form of the distribution function is applied to the Vlasov equation and its consequence to the QSS is examined, but the in-depth details are different. The major difference is that they applied the analysis to the regime in which the QSS did not differ much from the

initial state. In our case, we start from the far out-of-equilibrium initial state. Hence, our analysis does not aim to describe the detailed phase-space density distribution of the QSS via δf , but we only describe how far the global properties of the phase-space density of the QSS can deviate from the Vlasov limit. Another difference is that their work regarded the perturbations in the fluid limit while in our study, those perturbations represent the local finite- N fluctuations. Therefore, the resulting QSS from our analysis is the QSS with the finite- N effect involved and the test with the N -body simulations is straightforward.

III. SIMULATION DETAILS, INITIAL CONDITION AND UNITS

We test the hypothesis of the $1/N$ term that arises from the above analysis in the N -body simulations of one-dimensional self-gravitating system of particles of identical mass m . This model is also known as the self-gravitating sheet model. The Newtonian gravitational acceleration from the particle j located at x_j acting on the particle i at x_i reads

$$a_{ji} = gm \frac{x_j - x_i}{|x_j - x_i|} \quad (7)$$

where g is the gravitational constant. The force expressed in Eq. (7) is the mutual attractive constant force regardless of separation. This facilitates the numerical integrations of the equations of motion of particles as they can be carried out in the exact way up to the crossing where the forces on the encountering particles have to be re-determined. The most optimized algorithm to handle this is the heap-based algorithm in which the crossing times of all pairs of adjacent particles are stored and managed in a data heap [30]. The accuracy is such that the deviation of the total energy is comparable to the machine error at each crossing. At the end, the deviation of the total energy is less than $10^{-6}\%$.

For the initial condition, we adopt the rectangular waterbag configuration in phase space in which the initial position and velocity of particles are randomly distributed in the range of $(-x_0, x_0)$ and $(-v_0, v_0)$, with uniform probability. Thus, the uniform initial phase-space density (or f_0) inside the waterbag reads

$$f_0 = \frac{M}{4x_0v_0} \quad (8)$$

where $M = mN$ is the total mass and the phase-space density is zero outside. By this construction, the phase-space distribution is a two-level function which facilitates the analysis as f_0 is the integral of motion and it also indicates the maximum attainable phase-space density according to the LB theory. We choose to parameterize f_0 by the initial virial ratio $b_0 \equiv \frac{2T_0}{|U_0|}$, where T_0 and U_0 are the initial kinetic and potential energies of the system,

respectively, as

$$f_0 = \sqrt{\frac{M}{2gL^3b_0}} \quad (9)$$

where $L = 2x_0$ is the initial system size. Parameterizing the initial state by b_0 helps to identify easily how far the initial state is from the virial equilibrium. Throughout this study, we use a system of units where the gravitational constant g , the total mass M , and the system initial length L are unity. The unit of time t_d is chosen to be

$$t_d = \sqrt{\frac{L}{gM}} \quad (10)$$

which corresponds to the free-fall time of the $b_0 = 0$ system. After all particles are randomly sampled in phase space following the prescriptions above, we adjust all positions and velocities by the constants so that the center of mass is static at the origin. Relocating the center of mass in this way is equivalent to translating the waterbag in phase space while the initial degree of randomness, which is our central interest, is preserved.

Because we study the subtle effect from the random microscopic Poissonian fluctuations, which vary between realizations, to the macroscopic QSS, the simulation with a considerable number of realizations for each b_0 and N is preferable to obtain the dependable results. For this reason, we simulate 1000, 500, 250, 150, 100 and 50 different realizations for $N = 1000, 2000, 4000, 8000, 16000$ and 32000, respectively, and the ensemble average can be applied if necessary.

IV. NUMERICAL RESULTS

A. Waterbag evolution and phase-space density of QSS

In this section, we consider first of all the evolution of the waterbag. Shown in Fig. 1 is the evolution of the waterbag in phase space for $b_0 = 0.1$ and $N = 32000$, drawn from a single realization. The initial waterbag evolves to the QSS which, as seen at $300 t_d$, consists of a dense core and surrounding diluted halo achieved from wound filaments seen in the snapshots before. This kind of structure is known as the core-halo structure. The attainment to this structure can be described by the Vlasov dynamics as follows. In brief, the core phase-space density reflects the density of the initial waterbag, namely f_0 , while the filament densities do not. This is because filaments become finer while they are winding, lowering their coarse-grained phase-space density with time even though the fine-grained density is preserved to f_0 . On the contrary, the core does not stretch and wind, so its phase-space density remains at f_0 . The Vlasov description for the collisionless relaxation is deemed to be valid

until filaments become discontinuous due to limited resolution from finite N (see [31] for review). We observe that filaments are still intact until $80 t_d$. At $180 t_d$, they start to dissolve, but their trace in the halo is still observable. At $300 t_d$, filaments are more assimilated. We also spot a number of persistent holes in the halo, which emerge between the core and the winding filaments. The presence of phase-space holes does not significantly affect the analysis because they are situated well outside the core, whereas we will examine the core to test our hypothesis of the $1/N$ term.

From the visual inspection of the waterbag evolution, we continue with an inspection of the phase-space density distribution of the QSS. Shown in Fig. 2 is the ensemble-averaged phase-space density as a function of the energy per unit mass $f(\epsilon)$ at $300 t_d$ for $b_0 = 0.3$ and 0.8 , and for various N . To compute $f(\epsilon)$, we first determine the energy distribution of particles $F(\epsilon)$ such that $\int F(\epsilon)d\epsilon = M$. Then, the conversion of the distribution from the energy domain (or $F(\epsilon)$) to the phase-space domain (or $f(\epsilon)$) is carried out by the relation

$$F(\epsilon) = g(\epsilon)f(\epsilon) \quad (11)$$

where $g(\epsilon)$ is the density of state at energy ϵ which can be computed from

$$g(\epsilon) = \int_{\Phi_0}^{\epsilon} \frac{2\sqrt{2}}{a(\Phi)\sqrt{\epsilon - \Phi}} d\Phi. \quad (12)$$

In Eq. (12), $a(\Phi) = \frac{d\Phi}{dx}$ is the magnitude of the acceleration. The lower integral limit Φ_0 corresponds to the minimum potential energy which is located at $x = 0$. For simplicity, we can set $\Phi_0 = 0$ without loss of generality. We determine the conversion factor $g(\epsilon)$ by the numerical integration of Eq. (12). The ensemble-averaged $f(\epsilon)$ is obtained by averaging $f(\epsilon)$ from each individual realization, accompanied with the error bars estimated from the standard deviation of the mean. In the plot, we provide f_0 for comparison. The advantage of inspecting the energy distribution in phase-space domain is that it can be directly compared to f_0 which is the conserved quantity in the collisionless evolution and indicates, in principle, the maximum attainable phase-space density. Thus, the degeneracy of the system and the deviation from that limit can be analyzed. In addition, the robustness of the ensemble-averaged $f(\epsilon)$ is tested by the bootstrapping method and the results are reported in Appendix A.

Because we aim to inspect the subtle properties of the QSS, to ascertain that the state at the end appropriately represents the QSS is crucial. On the one hand, we assure that the violent relaxation is put to an end well before that time. According to past studies, it was demonstrated that the violent relaxation that was probed by the virial ratio terminated within $100 t_d$ [32–34]. On the other hand, the fact that the collisional effect, which also originates from the finite- N fluctuations in the initial state according to the BBGKY hierarchy, is negligible for our conclusion is equally important. In a past research

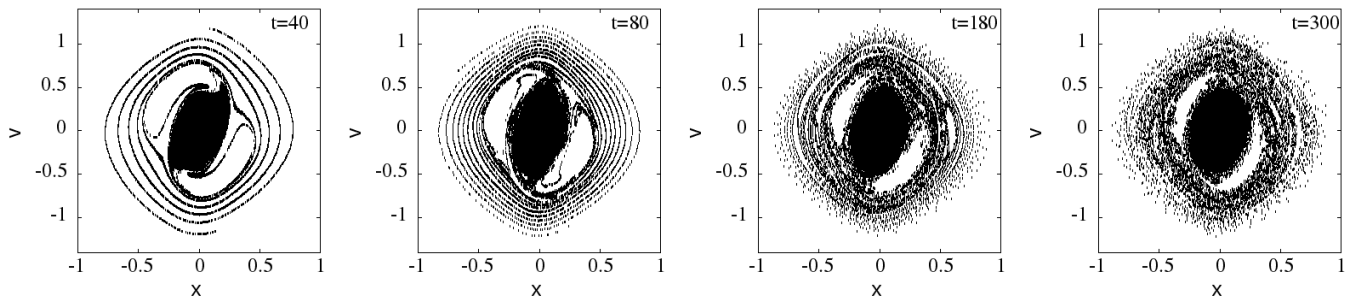


FIG. 1. Configurations in phase space for $b_0 = 0.1$ and $N = 32000$ at different times.

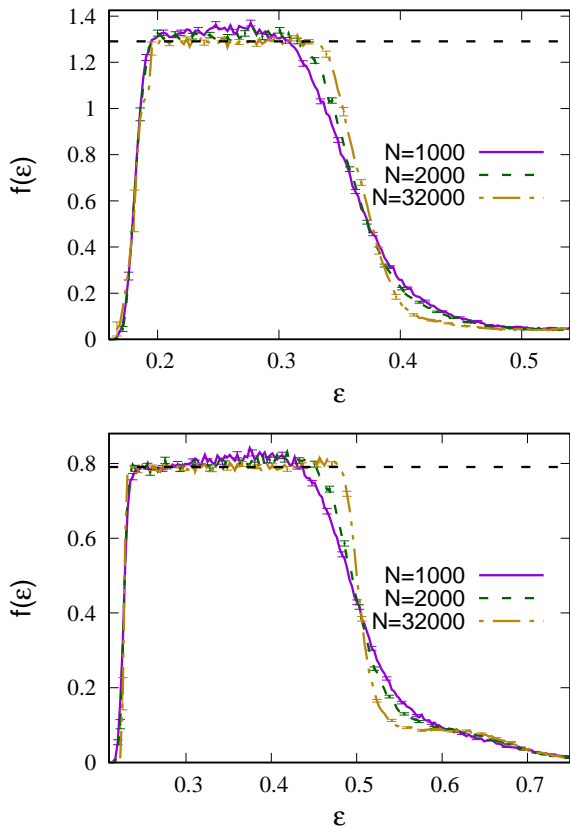


FIG. 2. Ensemble-averaged phase-space density as a function of the energy per unit mass $f(\epsilon)$ for $b_0 = 0.3$ (top panel) and 0.8 (bottom panel) and for different N . Plots are taken at $300 t_d$. Horizontal dashed line indicates the corresponding f_0 . Size of error bars corresponds to the standard deviation of the mean.

work [8], the collisional relaxation to thermal equilibrium was tracked by a set of order parameters which were defined to be zero at the thermal equilibrium and non-zero at the QSSs. The evolution of order parameters sug-

gested that the systems reached the QSS within $100 t_d$, in line with other studies, and remained in the QSSs for a long period of time. With $N = 800$, the order parameters saturated well in the QSSs and they did not start to evolve toward the thermal equilibrium earlier than $10^4 t_d$. In this study, we choose to inspect the systems with N higher than that case and the framed time scale is well before the collisional time scale. It is worth noting that the BBGKY hierarchy does not signify the total absence of the collisional effect in the time frame considered. The collisionality is also involved since the start as with our proposed $1/N$ term. Nevertheless, we can safely neglect the collisional effect for our results because, according to past studies, it becomes significant at much later time. Another point to be reassured is that, albeit the presence of persistent phase-space holes (see Fig. 1), $f(\epsilon)$ is well stationary in the last $100 t_d$, which is the time frame of consideration for further analysis.

From the $f(\epsilon)$ plot, the QSS exhibits two distinct components: the inner part has $f(\epsilon)$ close to f_0 while the outer part at higher ϵ has much lower density. This form corresponds to the core-halo structure as shown in Fig. 1 and the violent relaxation leading to such structure can be explained by the Vlasov equation. An alternative explanation for the fact that the core ends up in the degenerate state, which is the state of lowest possible energy, is given by the theory of the parametric resonance (see [35] for review). That theory was initially developed for explaining the halo formation in an ion system [36], but the adaptation to self-gravitating systems was also considered [37–40]. During the violent relaxation, quasi-periodic oscillation of potential field caused by a relaxing system can be in resonance with some particles. As a consequence, those particles gain the energy and are displaced further away, constituting the halo. The energy transfer halts when the core attains the degenerate state whose density is limited by f_0 . The parametric resonance in one-dimensional system was validated by the oscillation of the position of a test particle that was in phase with the system oscillation, so it was able to gain the energy and become part of halo [39, 41]. The fact that the core ends up in the LB degenerate state has been

verified in past works on the self-gravitating sheet model [20, 39, 42] and on other long-range interacting systems [38, 43], and our frame of work is based on that fact. Because the filaments are still intact at $\sim 80 t_d$, it is suggested that the parametric resonance takes place at the later time.

The continuum distribution function of the LB degenerate limit is the two-level step function given by

$$f(\epsilon) = \begin{cases} f_0, & \text{if } \Phi_0 < \epsilon < \epsilon_f \\ 0, & \text{otherwise} \end{cases} \quad (13)$$

where Φ_0 is the minimum energy and ϵ_f is the Fermi energy depending on the mass and f_0 . With a close inspection on the core phase-space density, we find that $f(\epsilon)$ can reach the value above f_0 and this excess is more noticeable for lower N . If N is higher, the core $f(\epsilon)$ is more uniform and closer to f_0 , albeit with fluctuations, and $f(\epsilon)$ falls more sharply to the halo level beyond the core energy limit. This implies that the core is closer to the LB degenerate $f(\epsilon)$. In fluid limit, the Vlasov equation suggests that the core distribution function takes the degenerate form (13). That the deviation from the degenerate distribution function is more evident if N is lower can be explained that the fluctuations of mean-field accelerations are higher in magnitude. This causes larger deviation of core particle trajectories from Vlasov mean-field trajectories. The phase-space density excess in Fig. 2 is out of the scope of the conventional violent relaxation theory because, according to the description by that theory, f_0 marks the maximum allowed phase-space density. We hypothesize that its origin is from the additional term in Eq. (5). It turns out that such term causes the QSS to be more concentrated than f_0 in phase space, specifically in the core part. Note that our study adopts a simple waterbag that consists of particles of identical mass and has a single uniform density, so a single core emerges. In a more complicated case, multiple cores can arise [44].

We remark that the phase-space distribution for $b_0 = 0.8$ and $N = 32000$ exhibits a plateau at high energy which contradicts the Penrose criterion from which a single maximum is allowed in the stationary state. We speculate that the emergence of this component is attributed to the parametric resonance that favors a certain range of the particle energy. These particles therefore constitute an overpopulated component at the high energy range. Another possibility is that, in continuity with the plot of phase-space configuration in Fig. 1, the underpopulated region is attributed to the voids that harbor no particles. Local maxima in the halo energy range were also spotted in past works [19, 45, 46] but this component was found to be meta-stable as it disappeared when the system reached the thermal equilibrium [8].

B. N -dependence of core phase-space density

In continuity with the observed excess of the phase-space density of the core in Sec. IV A, we will inspect it

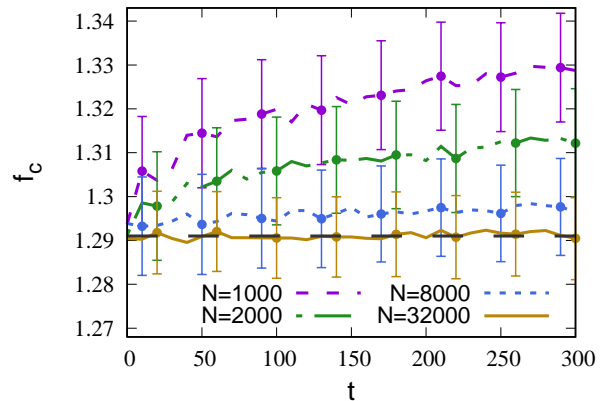


FIG. 3. Time evolution of the ensemble-averaged core phase-space density f_c for $b_0 = 0.3$ and for various N . Size of error bars is the average of the mean errors in the core region.

to a greater extent in this section. First of all, we verify if this excess is robust in the QSS and it is really achieved from the violent relaxation governed by mean field with fluctuations. To do so, we define the core phase-space density f_c to be the averaged $f(\epsilon)$ in the range of energy where $f > 0.99f_0$, and the time evolution of f_c for $b_0 = 0.3$ and for various N is plotted in Fig. 3. We observe that f_c increases from f_0 most prominently in the first 100 t_d which is during the violent relaxation. After 200 t_d , f_c saturates at the QSS. A system with low N tends to depart more from f_0 whereas for $N = 32000$, f_c remains close to f_0 all the time. This plot ascertains, firstly, that the QSS with the core phase-space density exceeding f_0 is a robust structure as a consequence of the violent relaxation. Secondly, the departure from the theoretical limiting value in the fluid limit during the violent relaxation is more noticeable in a lower N system. These are in line with the analytical result in Sec. II.

The deviation of f_c from f_0 can be investigated in a more quantitative way by defining

$$\Delta f \equiv \frac{f_c - f_0}{f_0} \quad (14)$$

to be the phase-space density excess of the core and the plot of the magnitude of the ensemble-averaged Δf (or $|\langle \Delta f \rangle|$) for different b_0 and N is shown in Fig. 4. The time average is also performed in the time window of width 50 t_d from 250 – 300 t_d to suppress the time fluctuations. The size of the error bars corresponds to the averaged mean errors in the same time window. For each N , $|\langle \Delta f \rangle|$ tends to be higher when b_0 is lower, which implies that a further out-of-equilibrium initial state leads to a QSS that is further away from the Vlasov limit. A waterbag of lower b_0 collapses to the center more violently because of lower support from velocity dispersion. Thus, local fluctuations in the initial state gather more concentratedly in the core, leading to a more pronounced effect from the mean-field fluctuation term. Despite the variation in magnitude with b_0 , we observe the decrease

of $|\langle \Delta f \rangle|$ with N for all b_0 . To verify if the decrease is in accordance with the $1/N$ estimate, we perform the curve-fitting with the $1/N^\gamma$ decay, where γ is a positive real number, for all b_0 and the results are depicted in Fig. 4. The line designating the $1/N$ decay is also put for comparison. The curve-fitting with the decreasing function that is not restricted to $1/N$ allows us to test the validity of the $1/N$ estimate properly and, if it is about to deviate from that estimate, to evaluate how large the discrepancy is. In all cases, the best-fitting γ is not far from 1. This affirms the reasonable applicability of the $1/N$ fluctuation term in the perturbed Vlasov equation that we proposed in Sec. II. While it is desirable if we keep increasing N and inspect further this finite- N effect, we foresee some limitations by doing so. For $N = 32000$, the deviation is of the order of a part per thousand or even below, and the deviation should be weaker if N is higher. Therefore, the capability to measure it properly is doubtful.

In past studies, the disagreement between the theoretical prediction of the QSS based on the continuum limit and the N -body simulations has been remarked in the HMF model (see, e.g., [11, 12]). Because that model is confined in a finite spatial domain, the stability analysis of the continuum distribution functions for the most probable state as the QSS is feasible. In our case, because a complete stability analysis to obtain the prediction of the QSS is not simple, we choose to infer from past studies that the core of the QSS follows the LB degenerate state. By our choice of initial conditions, the degenerate distribution function has a constant phase-space density equal to f_0 and we adopt it as the expected value. We not only find the discrepancy between the theory and the simulations as the past studies of the HMF model did, but we also attempt to understand better the origin of that discrepancy and its N -dependence. We are able to explain the cause of that deviation by the hypothesis of the $1/N$ term. If this $1/N$ term is generic for any long-range interacting systems, we speculate that the deviation of the measured parameters in the N -body system from the prediction in the fluid limit might scale with N in the same way as our result.

C. Core density profile and its agreement with LB theory

To inspect the core in more details, the ensemble-averaged density profile of the core $\rho(x)$ is plotted in Fig. 5 for some selected b_0 and N . We define the core to be the component below ϵ_c at which $f(\epsilon)$ falls to $0.99f_0$. We provide the corresponding density profile of the LB degenerate limit for comparison, which is numerically calculated from the distribution function (13) via the Poisson equation. The plot of the LB density profile in Fig. 5 is obtained by averaging the LB profiles calculated from the core mass of each realization. The bootstrapping test for the robustness of the core density profile is also per-

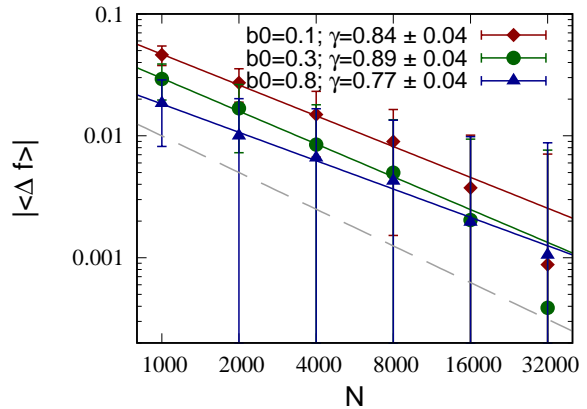


FIG. 4. Magnitude of the averaged Δf (or $|\langle \Delta f \rangle|$) as a function of N for different b_0 . The solid line is the best-fitting $1/N^\gamma$ function with the best-fitting γ reported for each case. The dashed line is the $1/N$ decay for comparison. Size of error bars corresponds to the averaged mean error in that time window.

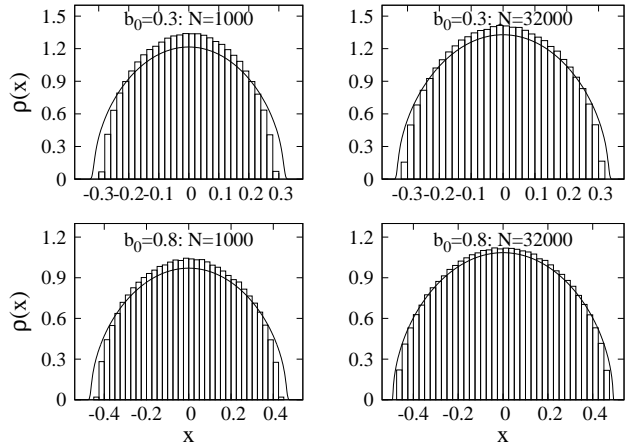


FIG. 5. Density profile of the core $\rho(x)$ for $b_0 = 0.3$ (two top panels) and 0.8 (two bottom panels) in histogram. For each b_0 , we depict $\rho(x)$ for $N = 1000$ and 32000 . Solid line is the averaged density profile of the LB degenerate limit.

formed and the results are reported in Appendix A. From the plot, the deviation from the LB degenerate limit is remarkable when one inspects the density profile although $|\langle \Delta f \rangle|$ is as small as a few percents or sub-percent. For $b_0 = 0.3$, the simulated core is evidently more concentrated than the degenerate limit counterpart. These two profiles become closer to each other if N increases from 1000 to 32000. For $b_0 = 0.8$, the over-dense core is also observed for $N = 1000$ but the discrepancy is not as large as in the $b_0 = 0.3$ plot for the same N . As N reaches 32000, the simulated and theoretical profiles almost coincide. That the core density profile becomes closer to the LB degenerate limit for higher N is in coherence with the $f(\epsilon)$ plots in Fig. 2. The plots in Fig. 5 are another evidences of the influence of the proposed $1/N$ term that

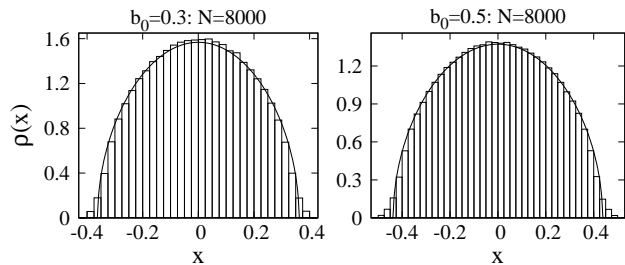


FIG. 6. Density profile of the central component $\rho(x)$ below the energy $\epsilon_{c,10}$ at which $f(\epsilon)$ falls to $0.1f_0$ for $b_0 = 0.3$ (left panel) and 0.5 (right panel), both of which have 8000 particles. Solid line represents the density profile of the LB degenerate limit for the corresponding f_0 and the mass of this component.

deviates the core from the continuum degenerate limit. In past studies, a reasonable agreement between the simulated QSS and the LB profile has been captured for b_0 close to 1 [19, 20]. In this work, we prove further that the agreement with the LB theory, albeit delimited to the core, improves if we increase N . That tendency is found even if b_0 is considerably far from 1. Note that a better agreement for a higher N system may not be realized if we consider the entire system because the situation is not simple. This is because the underlying parametric resonance that brings the core to the degenerate state, on the other hand, decouples the halo from the core. Thus, the entire system is not fully mixed. This scenario is recognized as the incomplete relaxation which prevents the QSS to take the LB form [47]. Another possibility of the incomplete relaxation is that the systems consist of particles of different masses. This leads to the mass segregation which also prevents the system to be fully relaxed [16, 17].

Finally, we revisit the ansatz of Teles et al (2011) [39] which proposed that the core-halo structure can be well fitted by the three-level distribution function. In that ansatz, the core phase-space density is fixed to f_0 while the constant halo phase-space density, the core energy limit and the halo energy limit are determined self-consistently by the mass and energy constraints, and the energy of the furthest particle. Otherwise, the distribution function is zero. Our results make evident that the simulated $f(\epsilon)$ is more complex than the three-level configuration (see Fig. 2). We note the intermediate region where $f(\epsilon)$ decreases from the core density to the halo density that spans a considerable range of ϵ , and we also note that the profile of this region varies considerably with N . Furthermore, we have inspected the density profile of the core that is restricted to be within the near-degenerate central region and a poor agreement with the LB degenerate distribution function has been observed in most cases. It is nevertheless worth testing that ansatz for the simulated core whether the agreement improves if we escalate the core energy limit from

the value adopted in past sections while the core phase-space density is still fixed to f_0 . To do this, we shift the core cutoff energy to the intermediate region at which $f(\epsilon)$ falls to $0.1f_0$, i.e., $\epsilon_{c,10}$, in the attempt to average the over-dense core and a part of less dense intermediate region. The density profile of the core which is now constituted from the particles with energies below $\epsilon_{c,10}$ and the corresponding LB degenerate profile are plotted in Fig. 6 for $b_0 = 0.3$ and 0.5 , both of which comprise 8000 particles that are comparable to the original work of Teles et al (2011) [39]. We observe a good agreement with the LB degenerate density profiles of these central components. Although we do not investigate further the full core-halo distribution function, our result affirms the applicability of the two-level function, with modified energy limit, to the central component. The agreement found in the $b_0 = 0.5$ plot is in accordance with [39] whereas we prove that the agreement can be found even though b_0 is significantly below. We note a density tail beyond the LB profile and it is the part that exhibits an obvious inconsistency. We speculate that it originates from the fluctuations of the energies of particles near the cutoff energy as the particles merely inside the degenerate profile can possibly have the energies higher than the cutoff energy, which are then excluded from the consideration, and vice versa for the particles merely outside. Despite this good agreement with numerical results, we may have a different opinion because the importance of the finite- N effect might be overlooked. We demonstrate that such effect causes the evident variation with N of the core. This implies the violation of the collisionless Vlasov equation due to the finite- N effect that should be of concern.

V. CONCLUSION

We have investigated the significance of the local finite- N fluctuations embedded in the initial states of systems of particles to the QSS that marks the end of a violent relaxation. Based on the conventional mean-field description of the violent relaxation, the particle number N has no influence on either the violent relaxation time scale or the statistical description of the QSS. We have identified the finite- N contribution in the Vlasov equation as the local mean-field fluctuation term proportional to $1/N$. This term is intrinsically different from the collision term since it is of mean-field origin unlike the collision term that involves the two-body interaction. Therefore, this term is effective in the violent relaxation in the way that it deviates the system from the Vlasov limit at a rate proportional to $1/N$. This implies the N -dependent QSS in the way that the deviation degree from the Vlasov limit is scaled by $1/N$.

That hypothesis is tested in the simulations of one-dimensional self-gravitating systems starting from a simple waterbag initial condition of constant phase-space density f_0 . The phase-space density distribution is a two-

level function: it is equal to f_0 inside the waterbag and 0 elsewhere. In this way, f_0 can serve as a reference of the degeneracy. We focus on the core of the QSS which, according to past studies, typically attains the LB degenerate state as a result of the parametric resonance during the violent relaxation. The LB degenerate limit designates the state of lowest possible energy in the fluid limit and it is unique to f_0 and mass. We find that the core phase-space density can exceed f_0 which marks the maximum attainable value according to the conventional violent relaxation theory. By a proper measurement of the phase-space density excess, we find that the deviation is in agreement with the $1/N$ estimate. A larger deviation from the Vlasov limit in a system of lower N is further affirmed by the inspection of the core density profile where the agreement between the simulated core density profile and the LB degenerate density profile improves for higher N . In conclusion, we underline the importance of the correction term in the Vlasov equation when dealing with N -body systems. Although our study

provides a reasonably precise description of the $1/N$ term that is applicable to the core, the detail of the entire QSS remains to be resolved.

ACKNOWLEDGMENTS

This research has received funding support from the National Science, Research and Innovation Fund (NSRF) via the Program Management Unit for Human Resources & Institutional Development, Research and Innovation (PMUB) (grant number B05F640075), and partly by Thailand Science Research and Innovation (TSRI) via Suranaree University of Technology (SUT) (grant number 179349). Numerical simulations are facilitated by HPC resources of the National Astronomical Research Institute of Thailand (NARIT). The author also thanks useful comments from anonymous reviewers and C. Herold in improving the manuscript.

-
- [1] A. Campa, T. Dauxois, and S. Ruffo, *Phys. Rep.* **480**, 57 (2009).
- [2] D. Lynden-Bell, *Mon. Not. R. Astr. Soc.* **136**, 101 (1967).
- [3] W. Braun and K. Hepp, *Commun. Math. Phys.* **56**, 101 (1977).
- [4] P. H. Chavanis, *J. Stat. Mech. Theory Exp.* **5**, 19 (2010).
- [5] J.-B. Fouvry and B. Bar-Or, *Mon. Not. R. Astr. Soc.* **481**, 4566 (2018).
- [6] B. N. Miller, *Phys. Rev. E* **53**, R4279 (1996).
- [7] T. Tsuchiya, N. Gouda, and T. Konishi, *Phys. Rev. E* **53**, 2210 (1996).
- [8] M. Joyce and T. Worrakitpoonpon, *J. Stat. Mech. Theory Exp.* **10**, 10012 (2010).
- [9] Y. Y. Yamaguchi, *Phys. Rev. E* **68**, 066210 (2003).
- [10] K. Jain, F. Bouchet, and D. Mukamel, *J. Stat. Mech. Theory Exp.* **2007**, 11008 (2007).
- [11] Y. Y. Yamaguchi, J. Barré, F. Bouchet, T. Dauxois, and S. Ruffo, *Physica A* **337**, 36 (2004).
- [12] A. Antoniazzi, F. Califano, D. Fanelli, and S. Ruffo, *Phys. Rev. Lett.* **98**, 150602 (2007).
- [13] A. Campa and P.-H. Chavanis, *Journal of Statistical Mechanics: Theory and Experiment* **5**, 013201 (2017).
- [14] A. Santini, G. Giachetti, and L. Casetti, *J. Stat. Mech. Theory Exp.* **2022**, 013210 (2022).
- [15] A. Gabrielli, M. Joyce, and J. Morand, *Phys. Rev. E* **90**, 062910 (2014), arXiv:1408.0999 [cond-mat.stat-mech].
- [16] K. R. Yawn and B. N. Miller, *Phys. Rev. Lett.* **79**, 3561 (1997).
- [17] K. R. Yawn and B. N. Miller, *Phys. Rev. E* **68**, 056120 (2003).
- [18] I. Arad and D. Lynden-Bell, *Mon. Not. R. Astr. Soc.* **361**, 385 (2005).
- [19] Y. Y. Yamaguchi, *Phys. Rev. E* **78**, 041114 (2008).
- [20] M. Joyce and T. Worrakitpoonpon, *Phys. Rev. E* **84**, 011139 (2011).
- [21] F. P. C. Benetti and B. Marcos, *Phys. Rev. E* **95**, 022111 (2017).
- [22] P.-H. Chavanis, *Physica A* **606**, 128089 (2022).
- [23] P. H. Chavanis, *Physica A* **387**, 787 (2008).
- [24] G. Janin, *Astron. Astrophys.* **11**, 188 (1971).
- [25] P. de Buyl and P. Gaspard, *Phys. Rev. E* **84**, 061139 (2011), arXiv:1108.0728 [cond-mat.stat-mech].
- [26] S. Colombi and J. Touma, *Mon. Not. R. Astr. Soc.* **441**, 2414 (2014).
- [27] S. Colombi, *Mon. Not. R. Astr. Soc.* **446**, 2902 (2015).
- [28] E. I. Barnes and R. J. Ragan, *Mon. Not. R. Astr. Soc.* **437**, 2340 (2014).
- [29] R. J. Ragan and E. I. Barnes, *Mon. Not. R. Astr. Soc.* **487**, 3618 (2019).
- [30] D. Fanelli, A. Noullez, and E. Aurell, *J. Comp. Phys.* **186**, 697 (2003).
- [31] B. Miller, G. Manfredi, D. Pirjol, and J.-L. Rouet, *Class. Quantum Grav.* **40**, 073001 (2023).
- [32] M. Luwel, G. Severne, and P. J. Rousseeuw, *Astrophys. Space Sci.* **100**, 261 (1984).
- [33] P. Mineau, M. R. Feix, and J. L. Rouet, *Astron. Astrophys.* **228**, 344 (1990).
- [34] P. Mineau, J. L. Rouet and M. R. Feix, *Phys. Rev. E* **59**, 73 (1999).
- [35] Y. Levin, R. Pakter, F. B. Rizzato, T. N. Teles, and F. P. C. Benetti, *Phys. Rep.* **535**, 1 (2014).
- [36] R. L. Gluckstern, *Phys. Rev. Lett.* **73**, 1247 (1994).
- [37] Y. Levin, R. Pakter, and T. N. Teles, *Phys. Rev. Lett.* **100**, 040604 (2008).
- [38] Y. Levin, R. Pakter, and F. B. Rizzato, *Phys. Rev. E* **78**, 021130 (2008).
- [39] T. N. Teles, Y. Levin, and R. Pakter, *Mon. Not. R. Astron. Soc.* **417**, L21 (2011).
- [40] R. Pakter and Y. Levin, *Phys. Rev. Lett.* **106** (2011).
- [41] T. Tashiro, *Physics Letters A* **383**, 125829 (2019), arXiv:1903.03307 [cond-mat.stat-mech].
- [42] M. Lecar and L. Cohen, *Astrophys. Space Sci.* **13**, 397 (1971).
- [43] T. N. Teles, Y. Levin, R. Pakter, and F. B. Rizzato, *J. Stat. Mech. Theory Exp.* **05**, 05007 (2010).

- [44] C. Reidl and B. N. Miller, Phys. Rev. E **51**, 884 (1995).
- [45] F. Hohl and M. Feix, Astrophys. J. **147**, 147 (1967).
- [46] T. Yamashiro, N. Gouda, and M. Sakagami, Progress of Theoretical Physics **88**, 269 (1992).
- [47] P.-H. Chavanis, Physica A **365**, 102 (2006).

Appendix A: Bootstrapping test for the QSS

In this appendix, we report the results of the bootstrapping test for the robustness of the QSS. We choose the cases with $b_0 = 0.1$ and $N = 1000$, which is furthest away from the Vlasov limit, and $b_0 = 0.1$ and $N = 32000$,

which has the lowest number of realizations. We compute the phase-space density distribution $f(\epsilon)$ (Fig. 7) and the density profile of the core $\rho(x)$ (Fig. 8) for 5 different subsamples. The horizontal line denoting f_0 is also provided in the $f(\epsilon)$ plots. In each subsample, 20% of the realizations are randomly pulled off. Although the variation of the QSS among realizations is expected, especially for cases with low N , both figures ascertain that the number of realizations for our study is sufficient to yield the dependable results as the computed profiles almost coincide.

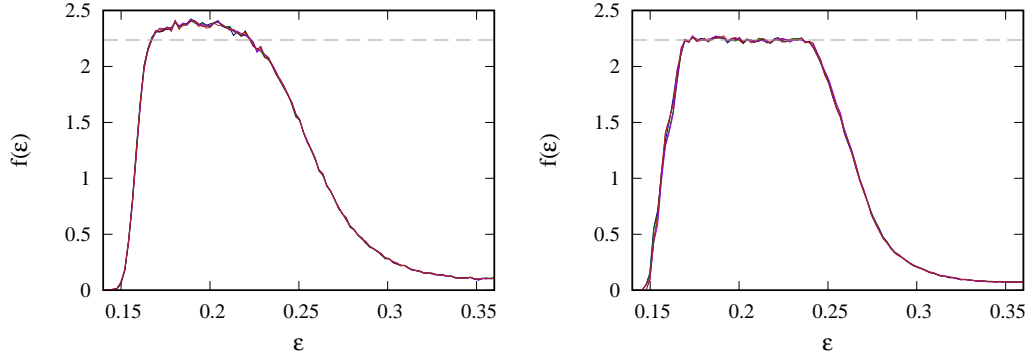


FIG. 7. Phase-space density distribution $f(\epsilon)$ for $b_0 = 0.1$ and $N = 1000$ (left panel) and $b_0 = 0.1$ and $N = 32000$ (right panel) for 5 different subsamples, each of which consists of randomly chosen 80% of realizations. The horizontal dashed line indicates the value of f_0 .

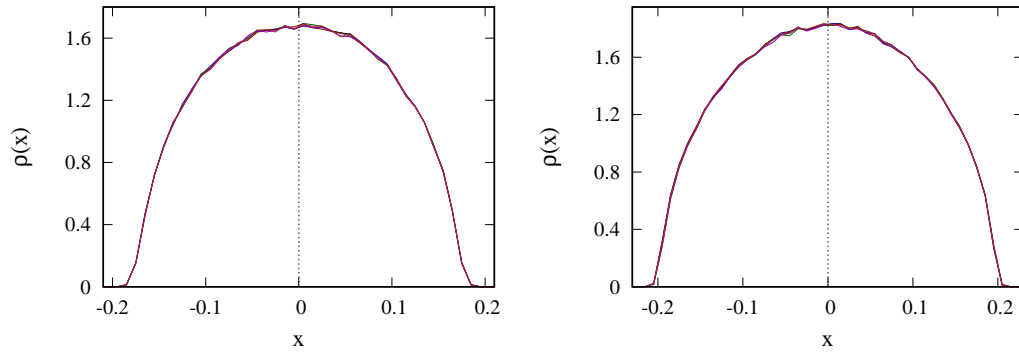


FIG. 8. Density profile of the core $\rho(x)$ for $b_0 = 0.1$ and $N = 1000$ (left panel) and $b_0 = 0.1$ and $N = 32000$ (right panel) for 5 different subsamples, each of which consists of randomly chosen 80% of realizations.